PAI-1 secreted from metastatic ovarian cancer cells triggers the tumor-promoting role of the mesothelium in a feedback loop to accelerate peritoneal dissemination

Yang Peng[1], Hiroaki Kajiyama[1*], Hong Yuan[1], Kae Nakamura[1], Masato Yoshihara[1], Akira Yokoi[1], Kayo Fujikake[1], Hiroaki Yasui[1], Nobuhisa Yoshikawa[1], Shiro Suzuki[1], Takeshi Senga[2], Kiyosumi Shibata[3], Fumitaka Kikkawa[1]

[1] Department of Obstetrics and Gynecology, Graduate School of Medicine, Nagoya University, Showa-ku, Nagoya 466-8550, Japan.

[2] Department of Internal Medicine, Yahagigawa Hospital, Anjyo 444-1164, Aichi, Japan.

[3] Department of Obstetrics and Gynecology, Banbuntane Hotokukai Hospital, Fujita Health University, Nakagawa-ku, Nagoya 454-8509, Aichi, Japan.

[*] Correspondence and requests for materials should be addressed to Hiroaki Kajiyama (Kajiyamah@gmail.com)

Archive and Access to this publication: https://doi.org/10.1016/j.canlet.2018.10.027

Abstract

The mesothelium, covered by a continuous monolayer of mesothelial cells, is the first protective barrier against metastatic ovarian cancer. However, mesothelial cells release tumor-promoting factors that accelerate the process of peritoneal metastasis. We identified cancer-associated mesothelial cells (CAMs) that had tumor-promoting potential. Here, we found that plasminogen activator inhibitor-1 (PAI-1) induced the formation of CAMs, after which CAMs increasingly secreted the oncogenic factors interleukin-8 (IL-8) and C-X-C motif chemokine ligand 5 (CXCL5), further promoting the metastasis of ovarian cancer cells in a feedback loop. After the formation of CAMs, PAI-1 activated the nuclear factor kappa B (NFκB) pathway in the CAMs, thus transcriptionally upregulating the expression of the downstream NFκB targets IL-8 and CXCL5. Moreover, PAI-1 correlated with peritoneal metastasis in ovarian cancer patients and indicated a poor prognosis. In both *ex vivo* and *in vivo* models, after PAI-1 expression was knocked down, the metastasis of ovarian cancer cells decreased significantly. Therefore, targeting PAI-1 may provide a potential target for future therapeutics to prevent the formation of CAMs and alleviate peritoneal metastasis in ovarian cancer patients.

Key words: ovarian cancer; cancer-associated mesothelial cells; plasminogen activator inhibitor-1; peritoneal metastasis; microenvironment.

1. Introduction

More than 70% of ovarian cancer patients are initially diagnosed at advanced FIGO stages [1]. Peritoneal metastasis is life-threatening for advanced FIGO stage patients, and the survival rate is less than 50% [2]. Peritoneal metastasis of ovarian cancer is different from metastases of other types of cancers because the method of metastasis is unique: the ovarian cancer cells spread directly to the peritoneal cavity [3]. The peritoneal microenvironment contains enzymes, cytokines, and chemokines that are responsible for the regulation of tumor metastasis [4, 5]. Sphingosine-1-phosphate (S1P), interleukin-8 (IL-8), and vascular endothelial growth factor (VEGF) are abundant in ascites from ovarian cancer patients. These factors regulate cancer cell dissemination [6-9].

Human peritoneal mesothelial cells (HPMCs) have played important roles in the microenvironment of ovarian cancer metastasis [10-13]. As the front line for protection, HPMCs are a defensive barrier against cancer cells. *Michihiko N et al.* found that hepatocyte growth factor (HGF) secreted from ovarian cancer cells induced the mesothelial-mesenchymal transition (MMT) of HPMCs [14]. MMT of mesothelial cells makes the dissemination of ovarian cancer cells much easier because the tight mesothelium cell barrier is disrupted [15-17]. Meanwhile, oncogenic factors released by HPMCs are deleterious and accelerate tumor progression [12]. For example, lipoprotein-A (LPA) is constitutively produced by the mesothelium, increasing the chemotactic activity of metastatic ovarian cancer [18]. Cancer-associated fibroblasts (CAFs) are drivers of tumorigenicity in cancer cells due to multicellular and stromal-dependent alterations [19, 20]. Based on this, the tumor-promoting mesothelial cells in one of our previous studies were called cancer-associated mesothelial cells (CAMs) [21]. The transformation from HPMCs to CAMs and the underlying mechanism attracted our interest.

Plasminogen activator inhibitor-1 (PAI-1) was initially known as an inhibitor of fibrinolysis by inhibiting the proteolytic activity of tissue-type plasminogen activator

(tPA) and urokinase-type plasminogen activator (u-PA) [22]. The inhibition of PAI-1 leads to an increase of thrombolysis in artery disease [23, 24]. Both dependent on and independent of its protease inhibitory effect, PAI-1 regulates cellular activities in lung, renal and breast cancers [25-27]. Aside from regulating the fibrinolytic system in cancer, PAI-1 independently and directly mediates cancer cell proliferation and migration [28]. However, the role of PAI-1 in metastatic ovarian cancer remains unknown.

Here, we determined how HPMCs switched from their barrier function into CAMs and how CAMs promoted cancer metastasis. PAI-1 was a crucial regulator of ovarian cancer-mesothelium crosstalk. PAI-1 secreted from metastatic ovarian cancer cells triggered the CAM transition. In response, CAMs provided a pro-metastatic effect on the cancer cells. As a result, a feedback loop was gradually formed, making it easier for ovarian cancer cells to disseminate.

2. Materials and Methods

2.1 Tissue samples

A total of 67 cases of paraffin-embedded ovarian cancer samples were obtained from patients who underwent surgical resection at Nagoya University Hospital from 1992 to 2010. It was approved by the Ethics Committee of Nagoya University Hospital (in accordance with the Declaration of Helsinki), with informed consent from all patients (approval number: 2017-0497). Histologic and diagnostic evaluations were performed by pathologists at the Pathology Diagnosis Center.

2.2 Cell culture

All ovarian cancer cell lines ES2, SKOV3 and HEY were purchased from American Type Culture Collection (ATCC, Manassas, VA, USA). With permission from the Ethics Committee (in accordance with the Declaration of Helsinki) and informed consent from patients (approval number: 2017-0497), HPMCs were

obtained from patients who underwent omentum resections and were diagnosed without malignancies. HPMCs were isolated as described previously [21]. RPM1-1640 (Sigma, USA) with 10% FBS (BI, Israel) was used for cell culture, in a humidified incubator at 37°C with 5% CO_2.

2.3 Antibodies and reagents

Except for the PAI-1 antibody (Proteintech, USA), all the other purified antibodies were purchased from Cell Signaling Technology ® (CST, USA): E-cadherin (#3195), N-cadherin (#13116), Vimentin (#5741), IKKα (#11930), IKKβ (#8943), p65 (#8242), ser536 (#3033), p50 (#3035), IκBα (#4814), LDH (#3582), and Lamin B (#12255). Recombinant PAI-1 was from PeproTech (Japan). PS1145 was from Sigma (USA). Tiplaxtinin was from Selleck (Osaka, Japan).

2.4 Protein extraction and Western blotting

Nuclear and cytoplasmic proteins were separated using a NE-PER Nuclear and Cytoplasmic Extraction Kit (#78833, Thermo, USA) according to the manufacturer's instructions. The protocol used for Western blotting was described previously [29].

2.5 RNA isolation and Real-Time quantitative PCR

Descriptions of total RNA isolation, reverse transcription, and RT-qPCR have been previously published by us [29]. The $2^{-\Delta\Delta Ct}$ method was used for calculation. All primers are presented in **Table S1** under **Supplementary Information 3.**

2.6 Immunohistochemistry, enzyme-linked immune-sorbent assay (ELISA), chromatin immunoprecipitation (ChIP) and other methods are described in **Supplementary Information 1.**

3. Results

3.1 PAI-1 is a key regulator inducing MMT in mesothelial cells.

To study the secretory effectors from metastatic ovarian cancer cells to the mesothelium, we cultured primary HPMCs with conditioned medium (supernatant from ovarian cancer cells). After 72 h, the shapes of the mesothelial cells became more mesenchymal-like **(Fig. 1A).** Western blotting demonstrated that E-cadherin expression was decreased and Vimentin was increased by conditioned medium, which indicated MMT was induced in HPMCs. Subsequently, these mesothelial cells were returned to normal culturing medium and incubated for another 72 h. We found that MMT was constantly maintained (**Fig. 1B, C**). A wound-healing assay indicated that the migratory ability of the mesothelial cells was promoted by the conditioned medium (**Fig. 1D**). These results indicated that MMT was induced by the conditioned medium.

Therefore, a cytokine antibody array was performed to identify the affecting candidates in the conditioned medium. PAI-1 was the most abundantly released factor in the supernatants from three ovarian cancer cell lines: ES2, SKOV3, and HEY cells (**Fig. 1E**). Western blotting and ELISA results showed high PAI-1 expression in these cells (**Fig. 1F, G**). Therefore, recombinant PAI-1 (15ng/mL) was used to directly stimulate the HMPCs. The wound-healing assay demonstrated that PAI-1 promoted the migratory ability of mesothelial cells in the same way that conditioned medium stimulated the migration of the cells (**Fig. 1H**). Thus, PAI-1 might be the most likely candidate in the conditioned medium to induce MMT in HPMCs.

3.2 An oncogenic feedback loop is formed after CAM formation triggered by PAI-1.

We assume that MMT might hint at CAM formation [12, 31]. To examine whether CAMs are transformed and, in turn, regulate ovarian cancer cells, we first initiated a CAM transition by treating HPMCs with either recombinant PAI-1 or conditioned medium for 72 h. Then, the supernatants were removed and replaced with fresh media (low FBS) for another 72 h. Finally, CAM supernatant, compared with HPMC

supernatant, was collected to treat ES2 and SKOV3 cells. Transwell assays demonstrated that in both ES2 and SKOV3 cells, migration and invasiveness were enhanced by the CAM supernatant (**Fig. 2A, B**). Thus, we performed a cytokine antibody array to identify the affecting cytokines. Compared with the supernatant from HPMCs, IL-8 and CXCL5 were concurrently upregulated in the supernatant from CAMs (**Fig. 2C**). An ELISA of the CAM supernatant further validated the upregulation of IL-8 and CXCL5, which might be the main cause of the tumor-promoting effect of CAMs (**Fig. 2D**). Secreted IL-8 in ovarian cancer promotes cancer metastasis both *in vitro* and *in vivo* [7, 32-34]. Similarly, CXCL5 is a pro-metastatic cytokine in ovarian cancer [35, 36]. When we removed PAI-1 from the HPMCS by using supernatants from ES2-shRNA cells (**Supplementary Fig. S1A-C**) instead, the increased secretion of IL-8 and CXCL5 from CAMs was significantly inhibited and the migration and invasion of ES2 and SKOV3 cells were unaffected, indicating CAM formation was efficiently blocked (**Supplementary Fig. S1D-F**). Therefore, we hypothesize that an oncogenic feedback loop is gradually formed, in which PAI-1 activates mesothelial cells to transform into CAMs so that they can promote the metastasis of cancer cells.

3.3 The nuclear NFκB pathway in CAMs is activated by PAI-1.

We investigated the underlying mechanism behind the dual up-regulation of IL-8 and CXCL5 in CAMs. Based on bio-informatics analysis (http://alggen.lsi.upc.es), we found that IL-8 and CXCL5 shared the same promoter binding region to NFκB (**Fig. 3A**). Therefore, we investigated whether NFκB pathway was activated in CAMs. Western blotting data demonstrated that nuclear p65 and ser536 (the phosphorylated form of p65) were increased after treatment with conditioned medium. IκBα and p50 remained unaffected. However, we did not find any changes to the expression of cytoplasmic proteins (**Fig. 3B**). Furthermore, recombinant PAI-1 was directly added to four independent cases of primary HPMCs. Although the level of ser536 was not

efficiently elevated in case #2, both nuclear p65 and ser536 were significantly increased in the other three cases，further validating the NFκB activation in different primary samples. These results also indicated that PAI-1 was a key stimulator of nuclear NFκB activation in CAMs (**Fig. 3C**). However, cytoplasmic protein expression was unaffected (**Supplementary Fig. S2A**). The activation of nuclear p65 and ser536 was also confirmed by immunofluorescence assays (**Supplementary Fig. S2B-C**).

Notably, we found that nuclear IKKβ expression was increased by PAI-1 (**Fig. 3B, C**). Inhibitors of nuclear factor κB kinase (IKKs), mainly IKKα and IKKβ, are upstream regulators of the NFκB pathway. IKKβ activates p65 by phosphorylating p65 at ser536 [37, 38]. Therefore, we pre-treated HPMCs with PS1145 (an IKKβ-specific inhibitor) for 24 h before PAI-1 treatment. Interestingly, we found that p65 was slightly activated by PAI-1 in CAMs even pretreated with PS1145. This demonstrated that the inhibitory effect of PS1145 was partially reversed following IKKβ re-activation induced by PAI-1 or CM. It was probably because other isoforms of IKKs also activated nuclear p65. However, the results still indicated that IKKβ was mainly responsible for PAI-1's regulation of NFκB (**Fig. 3D**). When we removed PAI-1 from the conditioned media (using ES2-shRNA cell supernatants), we found that nuclear NFκB activation in the mesothelial cells was repressed (**Fig. 3E**). Co-immunoprecipitation assays of the nuclear lysates showed that IKKβ phosphorylated p65 at ser536 by directly binding to it in the nucleus and PAI-1 increased these binding effects, resulting in NFκB activation (**Fig. 3F**). Overall, PAI-1 activated the nuclear NFκB pathway, at least partially via IKKβ-dependent regulation.

3.4 PAI-1 stimulation transcriptionally increases the recruitment of nuclear NFκB to the promoters of IL-8 and CXCL5.

The NFκB luciferase reporter assay was performed by co-transfection of HEK293T cells with the pTAL-NFκB vector (Firefly Luc) and the pRL-TK vector (Renilla Luc).

The results demonstrated that the luciferase activity of NFκB was significantly increased by PAI-1, indicating that PAI-1 directly accelerated the transcriptional activities of NFκB downstream cytokines (**Fig. 4A**).

In addition to IL-8 and CXCL5, tumor-necrosis-factor alpha (TNFα) and interleukin-6 (IL-6) are also canonical downstream cytokines of NFκB pathway and share a very similar binding sequence to that of IL-8 and CXCL5 (**Fig. 4B**). Therefore, we investigated the effects of PAI-1 stimulation on TNFα and IL-6 for comparison. After PAI-1 stimulation, IL-8 and CXCL5 mRNA expression was upregulated. However, TNFα and IL-6 mRNA expression was unaffected (**Fig. 4C**), which was consistent with that TNFα and IL-6 protein expression was not changed after CAM formation by cytokine antibody arrays **(Fig. 2C)**. Then, we performed the ChIP assay to examine the effects of direct promoter binding. We incubated p65, ser536, and IKKβ antibodies with lysates of PAI-1-induced CAMs. The results showed that PAI-1 significantly increased p65, ser536, and IKKβ recruitment to the promoters of IL-8 and CXCL5, but not to the TNFα and IL-6 promoters (**Fig. 4D**), suggesting that PAI-1 specifically activates the transcription of IL-8 and CXCL5. Subsequently, to investigate the regulatory role of IKKβ, we pre-treated mesothelial cells with PS1145 and performed the ChIP assay. The results revealed that IKKβ was required to upregulate p65 and ser536 binding to the IL-8 and CXCL5 promoters (**Fig. 4E**). Therefore, PAI-1 directly activated the transcription of IL-8 and CXCL5 by promoting the IKKβ-dependent recruitment of p65 and ser536 to their promoter regions.

3.5 Secretory PAI-1 activates CAM formation to accelerate ovarian cancer metastasis in both ex vivo and in vivo models.

To closely mimic the initial steps of peritoneal dissemination, we performed an *ex vivo* experiment [13, 39] involving human omentum samples from surgically treated patients. To fully understand the effect of secretory PAI-1, we stably inhibited PAI-1

in ES2-luc cells [30] using two shRNAs (**Supplementary Fig. S1**). These cells were seeded onto equally cut omentum pieces for co-incubation under normal cell culture conditions. The implanted cells were identified using the *in vivo* imaging system (IVIS) based on their bioluminescence values (**Fig. 5A**). After 3 days, both the ES2-sh1-luc and ES2-sh2-luc cells presented weakened implanting abilities (**Fig. 5B**). Therefore, we extended the *ex vivo* culture to 7 days, and introduced recombinant PAI-1. We found that PAI-1 significantly promoted cell metastasis under all conditions. When PAI-1 was inhibited, fewer cells resided on the omentum. However, this inhibition was reversed by the re-introduction of recombinant PAI-1 (**Fig. 5C**). Furthermore, all the omentum pieces were then digested by trypsin to extract the residing cancer cells. Then, these luc+ cells were quantified by the luciferase reporter assay. The results were consistent with those from the IVIS analysis (**Fig. 5D**). In addition, we established a co-culture model by seeding ES2-ZsGreen cells [30] onto a monolayer of primary HPMCs. Recombinant PAI-1 and tiplaxtinin (a PAI-1 inhibitor) were added to each group. PAI-1 significantly promoted the implantation of ovarian cancer cells (**Supplementary Fig. S3A**).

To study the role of CAMs *in vivo*, we co-injected (by intraperitoneal injection) ovarian cancer cells and primary mesothelial cells. Under the IVIS, the intraperitoneal tumor-bearing burden of each mouse was investigated. The total survival period after injection was less than 20 days. Due to the presence of mesothelial cells, peritoneal metastasis was severer than in mice injected solely with ovarian cancer cells. In dual injection groups, the metastasis-promoting effect was significantly repressed by the inhibition of PAI-1 secretion (**Fig. 5E**). The peritoneal resident tumor nodules in the mesenterium were compared, indicating that the presence of CAMs promoted peritoneal metastasis. When PAI-1 was repressed, the metastasis-promoting effect was alleviated (**Fig. 5F**). Lastly, the volume of ascites in the mice in each group was compared and it showed that human mesothelial cells increased the volume of mouse ascites; the tumor burden was alleviated by PAI-1 inhibition (**Fig. 5G**). These results

were further supported by direct observations of the mesenterium and omentum under the IVIS (**Supplementary Fig. S4B**). The body weight of each group showed no significant difference (**Supplementary Fig. S4C**).

Together, these results indicate that, in the development of peritoneal metastasis in ovarian cancer, the malignant role of CAMs is markedly promoted by PAI-1, accelerating the severity of the metastasis.

3.6 PAI-1 predicts poor clinical outcomes for ovarian cancer patients.

Last, we analyzed PAI-1 protein expression in tissue samples from Nagoya University (67 cases) and PAI-1 mRNA expression from The Cancer Genome Atlas (TCGA) database (586 cases). First, protein analysis by immunohistochemistry showed that all 67 patients positively expressed PAI-1. Using the *H*-score, PAI-1 expression was categorized as high (≥ 200) or low (< 200) (**Fig. 6A**). Kaplan-Meier analysis showed that upregulated PAI-1 predicted a poor survival rate among ovarian cancer patients ($P < 0.01$) (**Fig. 6B**). For the first time, we showed that a high level of PAI-1 was significantly correlated with peritoneal dissemination ($P < 0.01$) (**Table 1**). From TCGA database, we analyzed PAI-1 mRNA expression in 586 ovarian cancer patients. Compared with normal ovary tissues, PAI-1 was upregulated in cancer tissues. Of all the ovarian cancer cases, 61.95% exhibited a high expression of PAI-1. Likewise, PAI-1 was overexpressed in patients with late stage (III, IV) ovarian cancer ($P < 0.05$) (**Fig. 6C-E**). A high level of PAI-1 also predicted a poor survival rate in ovarian cancer patients ($P < 0.05$) (**Fig. 6F**). Furthermore, ELISA data showed that the PAI-1 level was higher in malignant ascites (n = 9) than in benign ascites (n = 13) (**Fig. 6G**).

In addition, univariate and multivariate analyses by Cox regression further confirmed that both PAI-1 protein ($P < 0.01$) and mRNA ($P < 0.05$) levels were independent risk predictors for overall survival (**Table S4-6** under **Supplementary Information 3**). Together, these data suggest that PAI-1 is of marked clinical

significance as an indicator of peritoneal metastasis and poor progression in ovarian cancer patients.

4. Discussion

The metastasis style of ovarian cancer is summarized as “seed and soil”. Detached from primary tumor sites, cancer cells (“seed”) flow directly into the peritoneal cavity and freely colonize secondary sites (“soil”) [40, 41]. Currently, many researchers are focusing on the primary site of ovarian cancer. However, the actual situation of peritoneal metastasis is not restricted to features of primary ovarian cancer sites. To a great extent, it involves the interaction of cancer cells with the local environment at the secondary sites [20]. Additionally, the liquid microenvironment provides an easier way to freely release mediators [42]. Secretory factors, such as cytokines, exosomes, and microvesicles, play crucial roles in intercellular regulation [43-45]. Our previous work demonstrated that exosomes promote ovarian cancer dissemination [46]. Here, we continued investigating secretory factors in the peritoneal microenvironment. A cytokine antibody array revealed many candidates; PAI-1 seemed the most likely candidate. Although PAI-1 promotes tumorigenesis in many cancers including ovarian cancer at the primary site [47], this is the first time it has been shown to regulate mesothelial cells at the secondary site. Conversely, mesothelial cells also release regulatory factors, such as oncogenic IL-8 and CXCL5, which affect the metastatic behavior of ovarian cancer cells. IL-8, IL-6, and growth-regulated oncogene-alpha (GRO-α) are upregulated in ascites, accelerating the invasiveness of ovarian cancer [34, 48, 49]. However, these types of mesothelial cells, which acquire tumor-promoting potential, were not clearly studied.

As the most superficial cell population in the peritoneal cavity, mesothelial cells are the first line of defense against cancer [16]. However, constantly stimulated by cancer-secreted mediators, mesothelial cells transform into cancer promoters or CAMs [21]. We characterized CAMs based on the supporting evidence: 1) MMT was

morphologically and functionally induced and constantly maintained in CAMs, physically providing a convenient pathway for cancer cell penetration and residence; 2) CAMs secreted pro-tumoral factors, such as IL-8 and CXCL5, to accelerate tumor metastasis; 3) CAMs promoted metastasis *in vitro* and tumor progression *in vivo*. To these ends, CAMs are crucially responsible for the acceleration of peritoneal metastasis.

We have identified some of the main features of CAMs. MMT is one important feature. Originating from EMT (epithelial-mesenchymal transition), MMT indicates that the tight bonding of continuous mesothelium is interrupted, thus providing an advantage for cancer cell dissemination [17]. As widely reported, TGF-β is one of the master molecules that induce EMT and is a strong activator of cancer-associated fibroblasts [4, 19, 50, 51]. HGF also promotes the implantation of ovarian cancer cells into the mesothelium via MMT [14]. However, our array results did not indicate TGF-β and HGF as potential candidates (**Fig. 1E**). Instead, PAI-1 was commonly overexpressed in the conditioned media we sampled. Furthermore, after PAI-1 stimulation, the HPMC phenotype became more mesenchymal-like, with a significantly elevated migratory ability. Thus, MMT indicates the change from HPMCs to CAMs.

Likewise, the activation of NFκB is another feature of CAMs. We focused on NFκB because its activation promotes a cascade of downstream cytokines; and IL-8 and CXCL5, which were increased simultaneously, share the same promoter binding region to NFκB. For the first time, PAI-1 was found to directly activate the transcription of NFκB downstream targets in mesothelial cells. We hypothesize that PAI-1, independent of its protease inhibitory activity, exhibits interactions with cellular surface of mesothelial cells to mediate NFκB activation. Regarding what PAI-1 binds to on the cell surface, PAI-1 is known to interact with low-density lipoprotein receptor-related protein 1 (LRP1), a receptor indirectly involved in NFκB signaling [52, 53]. Another hypothesis might be that PAI-1 increases the activation of

FLICE-like inhibitory protein (FLIP). FLIP is known to activate the downstream pathways of NFκB and ERK (extracellular signal-regulated kinase) to promote proliferation [54]. However, more study is needed to elucidate the mechanism behind PAI-1/NFκB regulation in CAMs. In particular, IKKβ directly bound to p65 and phosphorylated p65 at ser536 in CAM nuclei. In response to PAI-1, NFκB specifically activated the transcription of IL-8 and CXCL5, in which IKKβ is indispensable. However, even though IKKβ was inhibited by PS1145, the nuclear p65 was still slightly activated by PAI-1, indicating that besides IKKβ, probably other IKKs were involved into the PAI-1/NFκB activation (**Fig. 3D**). It was reported that IKKα phosphorylated p65 at ser536 [37]. IKKε knockdown presented an impaired phosphorylation of p65 at ser536, resulting in the NFκB inhibition [55]. Furthermore, cells expressed less IKKγ exhibited less NFκB activation, independent of IKKα expression [56]. Therefore, we pretreated mesothelial cells with a broad-spectrum IKKs inhibitor Bay117082, and found that p65 and ser536 were greatly inhibited, even PAI-1 stimulation was introduced (**Supplementary Fig. S5**). Based on these, we hypothesize that PAI-1's regulation of NFκB is at least partially via activating IKKβ.

CAM formation forms a pro-metastatic feedback loop, accelerating the pace of the peritoneal dissemination of ovarian cancer. PAI-1 is a key activator. When we blocked PAI-1 in ovarian cancer cells, the release of IL-8 and CXCL5 in CAMs was suppressed, indicating that CAM formation was blocked, and the feedback loop was partially cut off by PAI-1 inhibition. This is further demonstrated in our *in vivo* model. To better emphasize the role of mesothelial cells in the microenvironment, we performed an intraperitoneal co-injection of primary human mesothelial cells with ovarian cancer cells. The presence of human mesothelial cells worsened peritoneal metastasis *in vivo*. This observation is supported by the study by *Ksiazek K et al*, in which three ovarian cancer cell lines (SKOV3, A278, and OVCAR3 cells) were co-injected with mesothelial cells, and the role of CAMs was revealed. However, the factor triggering CAM formation remains unclear [11]. Here, we inhibited PAI-1

expression using shRNAs and found that the formation of CAMs was inhibited, and their pro-metastatic effect was significantly reduced. This suggests that PAI-1 is one of the essential triggering factors for CAM formation. Furthermore, in both *ex vivo* and co-culture models, which very closely reconstruct the environment of the peritoneum, PAI-1 significantly promoted the metastatic behavior of ovarian cancer cells.

Clinically, PAI-1 is upregulated in ovarian cancer tissues. A high level of PAI-1 independently indicates a poor prognosis in ovarian cancer patients [57]. Most importantly, PAI-1 is significantly correlated with peritoneal metastasis. For the first time, PAI-1 is described as a candidate for predicting tumor metastasis, and may be a promising diagnostic and prognostic marker. Surprisingly, PAI-1 was also associated with the recurrence of ovarian cancer (**Table 1**), which may be the focus of future studies.

In summary, this study illustrated the pro-metastasis feedback loop in the peritoneal microenvironment. Metastatic ovarian cancer cells activate the formation of CAMs by releasing PAI-1, which directly promotes NFκB activation to upregulate IL-8 and CXCL5 secretion from CAMs. IL-8 and CXCL5 further accelerate the progression of metastasis (**Supplementary Fig. S6**). Thus, targeting PAI-1 and blocking CAM formation in the loop could slow down the pace of ovarian cancer metastasis.

Conflicts of interest

All authors declare no conflicts of interest.

Appendix A. Supplementary data

Supplementary data related to this article can be found online at https://doi.org/10.1016/j.canlet.2018.10.027.

Acknowledgments

This work was supported by JSPS KAKENHI Grant (Number: 2617H04338). We also would like to thank Professor Yutaka Kondo and Dr. Miho Suzuki, Dr. Liang Weng, Dr. Peng Gu and Dr. Meng Zhao for their suggestions and warm help.

Reference

[1] B.T. Hennessy, R.L. Coleman, M. Markman, Ovarian cancer, Lancet (London, England), 374 (2009) 1371-1382.

[2] R.A. Smith, K.S. Andrews, D. Brooks, S.A. Fedewa, D. Manassaram-Baptiste, D. Saslow, O.W. Brawley, R.C. Wender, Cancer screening in the United States, 2017: A review of current American Cancer Society guidelines and current issues in cancer screening, CA: a cancer journal for clinicians, 67 (2017) 100-121.

[3] J. Mikula-Pietrasik, P. Uruski, A. Tykarski, K. Ksiazek, The peritoneal "soil" for a cancerous "seed": a comprehensive review of the pathogenesis of intraperitoneal cancer metastases, Cellular and molecular life sciences : CMLS, (2017).

[4] B. Thibault, M. Castells, J.P. Delord, B. Couderc, Ovarian cancer microenvironment: implications for cancer dissemination and chemoresistance acquisition, Cancer metastasis reviews, 33 (2014) 17-39.

[5] D.A. Leinster, H. Kulbe, G. Everitt, R. Thompson, M. Perretti, F.N. Gavins, D. Cooper, D. Gould, D.P. Ennis, M. Lockley, I.A. McNeish, S. Nourshargh, F.R. Balkwill, The peritoneal tumour microenvironment of high-grade serous ovarian cancer, The Journal of pathology, 227 (2012) 136-145.

[6] G. Hong, L.M. Baudhuin, Y. Xu, Sphingosine-1-phosphate modulates growth and adhesion of ovarian cancer cells, FEBS letters, 460 (1999) 513-518.

[7] M.M. Shahzad, J.M. Arevalo, G.N. Armaiz-Pena, C. Lu, R.L. Stone, M. Moreno-Smith, M. Nishimura, J.W. Lee, N.B. Jennings, J. Bottsford-Miller, P. Vivas-Mejia, S.K. Lutgendorf, G. Lopez-Berestein, M. Bar-Eli, S.W. Cole, A.K. Sood, Stress effects on FosB- and interleukin-8 (IL8)-driven ovarian cancer growth and metastasis, The Journal of biological chemistry, 285 (2010) 35462-35470.

[8] S. Bandaru, A.X. Zhou, P. Rouhi, Y. Zhang, M.O. Bergo, Y. Cao, L.M. Akyurek, Targeting filamin B induces tumor growth and metastasis via enhanced activity of matrix metalloproteinase-9 and secretion of VEGF-A, Oncogenesis, 3 (2014) e119.

[9] N. Ferrara, H.P. Gerber, J. LeCouter, The biology of VEGF and its receptors, Nature medicine, 9 (2003) 669-676.

[10] J. Mikula-Pietrasik, P. Uruski, P. Sosinska, K. Maksin, H. Piotrowska-Kempisty, M. Kucinska, M. Murias, S. Szubert, A. Wozniak, D. Szpurek, S. Sajdak, K. Piwocka, A. Tykarski, K. Ksiazek, Senescent peritoneal mesothelium creates a niche for ovarian cancer metastases, Cell death & disease, 7 (2016) e2565.

[11] J. Mikula-Pietrasik, P. Sosinska, M. Kucinska, M. Murias, K. Maksin, A. Malinska, A. Ziolkowska, H. Piotrowska, A. Wozniak, K. Ksiazek, Peritoneal mesothelium promotes the progression of ovarian cancer cells in vitro and in a mice xenograft model in vivo, Cancer letters, 355 (2014) 310-315.

[12] H.A. Kenny, C.Y. Chiang, E.A. White, E.M. Schryver, M. Habis, I.L. Romero, A. Ladanyi, C.V. Penicka, J. George, K. Matlin, A. Montag, K. Wroblewski, S.D. Yamada, A.P. Mazar, D. Bowtell, E. Lengyel, Mesothelial cells promote early ovarian cancer metastasis through fibronectin secretion, The Journal of clinical investigation, 124 (2014) 4614-4628.

[13] E. Lengyel, J.E. Burdette, H.A. Kenny, D. Matei, J. Pilrose, P. Haluska, K.P. Nephew, D.B. Hales, M.S. Stack, Epithelial ovarian cancer experimental models, Oncogene, 33 (2014) 3619-3633.

[14] M. Nakamura, Y.J. Ono, M. Kanemura, T. Tanaka, M. Hayashi, Y. Terai, M. Ohmichi, Hepatocyte growth factor secreted by ovarian cancer cells stimulates peritoneal implantation via the mesothelial-mesenchymal transition of the peritoneum, Gynecologic oncology, 139 (2015) 345-354.

[15] Y.J. Ono, M. Hayashi, A. Tanabe, A. Hayashi, M. Kanemura, Y. Terai, M. Ohmichi, Estradiol-mediated hepatocyte growth factor is involved in the implantation of endometriotic cells via the mesothelial-to-mesenchymal transition in the

peritoneum, American journal of physiology. Endocrinology and metabolism, 308 (2015) E950-959.

[16] R.A. Davidowitz, L.M. Selfors, M.P. Iwanicki, K.M. Elias, A. Karst, H. Piao, T.A. Ince, M.G. Drage, J. Dering, G.E. Konecny, U. Matulonis, G.B. Mills, D.J. Slamon, R. Drapkin, J.S. Brugge, Mesenchymal gene program-expressing ovarian cancer spheroids exhibit enhanced mesothelial clearance, The Journal of clinical investigation, 124 (2014) 2611-2625.

[17] P. Sandoval, J.A. Jimenez-Heffernan, G. Guerra-Azcona, M.L. Perez-Lozano, A. Rynne-Vidal, P. Albar-Vizcaino, F. Gil-Vera, P. Martin, M.J. Coronado, C. Barcena, J. Dotor, P.L. Majano, A.A. Peralta, M. Lopez-Cabrera, Mesothelial-to-mesenchymal transition in the pathogenesis of post-surgical peritoneal adhesions, The Journal of pathology, 239 (2016) 48-59.

[18] J. Ren, Y.J. Xiao, L.S. Singh, X. Zhao, Z. Zhao, L. Feng, T.M. Rose, G.D. Prestwich, Y. Xu, Lysophosphatidic acid is constitutively produced by human peritoneal mesothelial cells and enhances adhesion, migration, and invasion of ovarian cancer cells, Cancer research, 66 (2006) 3006-3014.

[19] P. Gascard, T.D. Tlsty, Carcinoma-associated fibroblasts: orchestrating the composition of malignancy, Genes & development, 30 (2016) 1002-1019.

[20] A. Rynne-Vidal, J.A. Jimenez-Heffernan, C. Fernandez-Chacon, M. Lopez-Cabrera, P. Sandoval, The Mesothelial Origin of Carcinoma Associated-Fibroblasts in Peritoneal Metastasis, Cancers, 7 (2015) 1994-2011.

[21] K. Fujikake, H. Kajiyama, M. Yoshihara, K. Nishino, N. Yoshikawa, F. Utsumi, S. Suzuki, K. Niimi, J. Sakata, H. Mitsui, K. Shibata, T. Senga, F. Kikkawa, A novel mechanism of neovascularization in peritoneal dissemination via cancer-associated mesothelial cells affected by TGF-beta derived from ovarian cancer, Oncology reports, 39 (2018) 193-200.

[22] R. Montesano, M.S. Pepper, U. Mohle-Steinlein, W. Risau, E.F. Wagner, L. Orci, Increased proteolytic activity is responsible for the aberrant morphogenetic behavior

of endothelial cells expressing the middle T oncogene, Cell, 62 (1990) 435-445.

[23] M. Schuliga, G. Westall, Y. Xia, A.G. Stewart, The plasminogen activation system: new targets in lung inflammation and remodeling, Current opinion in pharmacology, 13 (2013) 386-393.

[24] H.P. Kohler, P.J. Grant, Plasminogen-activator inhibitor type 1 and coronary artery disease, The New England journal of medicine, 342 (2000) 1792-1801.

[25] R. Ramer, A. Rohde, J. Merkord, H. Rohde, B. Hinz, Decrease of plasminogen activator inhibitor-1 may contribute to the anti-invasive action of cannabidiol on human lung cancer cells, Pharmaceutical research, 27 (2010) 2162-2174.

[26] W. Liu, H. Chen, N. Wong, W. Haynes, C.M. Baker, X. Wang, Pseudohypoxia induced by miR-126 deactivation promotes migration and therapeutic resistance in renal cell carcinoma, Cancer letters, 394 (2017) 65-75.

[27] M.P. Look, W.L. van Putten, M.J. Duffy, N. Harbeck, I.J. Christensen, C. Thomssen, R. Kates, F. Spyratos, M. Ferno, S. Eppenberger-Castori, C.G. Sweep, K. Ulm, J.P. Peyrat, P.M. Martin, H. Magdelenat, N. Brunner, C. Duggan, B.W. Lisboa, P.O. Bendahl, V. Quillien, A. Daver, G. Ricolleau, M.E. Meijer-van Gelder, P. Manders, W.E. Fiets, M.A. Blankenstein, P. Broet, S. Romain, G. Daxenbichler, G. Windbichler, T. Cufer, S. Borstnar, W. Kueng, L.V. Beex, J.G. Klijn, N. O'Higgins, U. Eppenberger, F. Janicke, M. Schmitt, J.A. Foekens, Pooled analysis of prognostic impact of urokinase-type plasminogen activator and its inhibitor PAI-1 in 8377 breast cancer patients, Journal of the National Cancer Institute, 94 (2002) 116-128.

[28] H. Fang, V.R. Placencio, Y.A. DeClerck, Protumorigenic activity of plasminogen activator inhibitor-1 through an antiapoptotic function, Journal of the National Cancer Institute, 104 (2012) 1470-1484.

[29] K. Nakamura, Y. Peng, F. Utsumi, H. Tanaka, M. Mizuno, S. Toyokuni, M. Hori, F. Kikkawa, H. Kajiyama, Novel Intraperitoneal Treatment With Non-Thermal Plasma-Activated Medium Inhibits Metastatic Potential of Ovarian Cancer Cells, Scientific reports, 7 (2017) 6085.

[30] K. Sugiyama, H. Kajiyama, K. Shibata, H. Yuan, F. Kikkawa, T. Senga, Expression of the miR200 family of microRNAs in mesothelial cells suppresses the dissemination of ovarian cancer cells, Molecular cancer therapeutics, 13 (2014) 2081-2091.

[31] P. Sandoval, J.A. Jimenez-Heffernan, A. Rynne-Vidal, M.L. Perez-Lozano, A. Gilsanz, V. Ruiz-Carpio, R. Reyes, J. Garcia-Bordas, K. Stamatakis, J. Dotor, P.L. Majano, M. Fresno, C. Cabanas, M. Lopez-Cabrera, Carcinoma-associated fibroblasts derive from mesothelial cells via mesothelial-to-mesenchymal transition in peritoneal metastasis, The Journal of pathology, 231 (2013) 517-531.

[32] H. Tong, J.Q. Ke, F.Z. Jiang, X.J. Wang, F.Y. Wang, Y.R. Li, W. Lu, X.P. Wan, Tumor-associated macrophage-derived CXCL8 could induce ERalpha suppression via HOXB13 in endometrial cancer, Cancer letters, 376 (2016) 127-136.

[33] T.J. Curiel, P. Cheng, P. Mottram, X. Alvarez, L. Moons, M. Evdemon-Hogan, S. Wei, L. Zou, I. Kryczek, G. Hoyle, A. Lackner, P. Carmeliet, W. Zou, Dendritic cell subsets differentially regulate angiogenesis in human ovarian cancer, Cancer research, 64 (2004) 5535-5538.

[34] A. Agarwal, S.L. Tressel, R. Kaimal, M. Balla, F.H. Lam, L. Covic, A. Kuliopulos, Identification of a metalloprotease-chemokine signaling system in the ovarian cancer microenvironment: implications for antiangiogenic therapy, Cancer research, 70 (2010) 5880-5890.

[35] J. Mikula-Pietrasik, P. Uruski, S. Szubert, R. Moszynski, D. Szpurek, S. Sajdak, A. Tykarski, K. Ksiazek, Biochemical composition of malignant ascites determines high aggressiveness of undifferentiated ovarian tumors, Medical oncology (Northwood, London, England), 33 (2016) 94.

[36] C.A. Cohen, A.A. Shea, C.L. Heffron, E.M. Schmelz, P.C. Roberts, The parity-associated microenvironmental niche in the omental fat band is refractory to ovarian cancer metastasis, Cancer prevention research (Philadelphia, Pa.), 6 (2013) 1182-1193.

[37] H. Sakurai, H. Chiba, H. Miyoshi, T. Sugita, W. Toriumi, IkappaB kinases phosphorylate NF-kappaB p65 subunit on serine 536 in the transactivation domain, The Journal of biological chemistry, 274 (1999) 30353-30356.

[38] B. Singha, H.R. Gatla, S. Manna, T.P. Chang, S. Sanacora, V. Poltoratsky, A. Vancura, I. Vancurova, Proteasome inhibition increases recruitment of IkappaB kinase beta (IKKbeta), S536P-p65, and transcription factor EGR1 to interleukin-8 (IL-8) promoter, resulting in increased IL-8 production in ovarian cancer cells, The Journal of biological chemistry, 289 (2014) 2687-2700.

[39] A.K. Mitra, C.Y. Chiang, P. Tiwari, S. Tomar, K.M. Watters, M.E. Peter, E. Lengyel, Microenvironment-induced downregulation of miR-193b drives ovarian cancer metastasis, Oncogene, 34 (2015) 5923-5932.

[40] M. Mendoza, C. Khanna, Revisiting the seed and soil in cancer metastasis, The international journal of biochemistry & cell biology, 41 (2009) 1452-1462.

[41] L. Mathot, J. Stenninger, Behavior of seeds and soil in the mechanism of metastasis: a deeper understanding, Cancer science, 103 (2012) 626-631.

[42] Z. Luo, Q. Wang, W.B. Lau, B. Lau, L. Xu, L. Zhao, H. Yang, M. Feng, Y. Xuan, Y. Yang, L. Lei, C. Wang, T. Yi, X. Zhao, Y. Wei, S. Zhou, Tumor microenvironment: The culprit for ovarian cancer metastasis?, Cancer letters, 377 (2016) 174-182.

[43] I. Matte, D. Lane, C. Laplante, C. Rancourt, A. Piche, Profiling of cytokines in human epithelial ovarian cancer ascites, American journal of cancer research, 2 (2012) 566-580.

[44] I. Matte, D. Lane, C. Laplante, P. Garde-Granger, C. Rancourt, A. Piche, Ovarian cancer ascites enhance the migration of patient-derived peritoneal mesothelial cells via cMet pathway through HGF-dependent and -independent mechanisms, International journal of cancer, 137 (2015) 289-298.

[45] L.M. Coussens, Z. Werb, Inflammation and cancer, Nature, 420 (2002) 860-867.

[46] A. Yokoi, Y. Yoshioka, Y. Yamamoto, M. Ishikawa, S.I. Ikeda, T. Kato, T.

Kiyono, F. Takeshita, H. Kajiyama, F. Kikkawa, T. Ochiya, Malignant extracellular vesicles carrying MMP1 mRNA facilitate peritoneal dissemination in ovarian cancer, Nature communications, 8 (2017) 14470.

[47] S. Mashiko, K. Kitatani, M. Toyoshima, A. Ichimura, T. Dan, T. Usui, M. Ishibashi, S. Shigeta, S. Nagase, T. Miyata, N. Yaegashi, Inhibition of plasminogen activator inhibitor-1 is a potential therapeutic strategy in ovarian cancer, Cancer biology & therapy, 16 (2015) 253-260.

[48] D. Milliken, C. Scotton, S. Raju, F. Balkwill, J. Wilson, Analysis of chemokines and chemokine receptor expression in ovarian cancer ascites, Clinical cancer research : an official journal of the American Association for Cancer Research, 8 (2002) 1108-1114.

[49] Y. Wang, L. Li, X. Guo, X. Jin, W. Sun, X. Zhang, R.C. Xu, Interleukin-6 signaling regulates anchorage-independent growth, proliferation, adhesion and invasion in human ovarian cancer cells, Cytokine, 59 (2012) 228-236.

[50] M. Wei, T. Yang, X. Chen, Y. Wu, X. Deng, W. He, J. Yang, Z. Wang, Malignant ascites-derived exosomes promote proliferation and induce carcinoma-associated fibroblasts transition in peritoneal mesothelial cells, Oncotarget, 8 (2017) 42262-42271.

[51] R.L. Elliott, G.C. Blobe, Role of transforming growth factor Beta in human cancer, Journal of clinical oncology : official journal of the American Society of Clinical Oncology, 23 (2005) 2078-2093.

[52] B. Degryse, J.G. Neels, R.P. Czekay, K. Aertgeerts, Y. Kamikubo, D.J. Loskutoff, The low density lipoprotein receptor-related protein is a motogenic receptor for plasminogen activator inhibitor-1, The Journal of biological chemistry, 279 (2004) 22595-22604.

[53] M. Luo, Y. Ji, Y. Luo, R. Li, W.P. Fay, J. Wu, Plasminogen activator inhibitor-1 regulates the vascular expression of vitronectin, Journal of thrombosis and haemostasis : JTH, 15 (2017) 2451-2460.

[54] Y. Chen, R.C. Budd, R.J. Kelm, Jr., B.E. Sobel, D.J. Schneider, Augmentation of proliferation of vascular smooth muscle cells by plasminogen activator inhibitor type 1, Arteriosclerosis, thrombosis, and vascular biology, 26 (2006) 1777-1783.

[55] C.V. Moser, K. Kynast, K. Baatz, O.Q. Russe, N. Ferreiros, H. Costiuk, R. Lu, A. Schmidtko, I. Tegeder, G. Geisslinger, E. Niederberger, The protein kinase IKKepsilon is a potential target for the treatment of inflammatory hyperalgesia, Journal of immunology (Baltimore, Md. : 1950), 187 (2011) 2617-2625.

[56] D.M. Rothwarf, E. Zandi, G. Natoli, M. Karin, IKK-gamma is an essential regulatory subunit of the IkappaB kinase complex, Nature, 395 (1998) 297-300.

[57] S. Chen, H. Tai, X. Tong, J. Wang, F. Yang, Y. Yang, O. Yiqin, Variation and prognostic value of serum plasminogen activator inhibitor-1 before and after chemotherapy in patients with epithelial ovarian cancer, The journal of obstetrics and gynaecology research, 40 (2014) 2058-2065.

[58] S.F. Faraj, A. Chaux, N. Gonzalez-Roibon, E. Munari, C. Ellis, T. Driscoll, M.P. Schoenberg, T.J. Bivalacqua, M. Shih Ie, G.J. Netto, ARID1A immunohistochemistry improves outcome prediction in invasive urothelial carcinoma of urinary bladder, Human pathology, 45 (2014) 2233-2239.

Figure legends

Figure 1. MMT is induced in mesothelial cells by conditioned medium, in which PAI-1 is a key regulator. (A) Morphological changes of primary mesothelial cells after being treated with conditioned medium from ovarian cancer cells (ES2). **(B)** After being stimulated by conditioned media (CM+), MMT markers were measured by Western blotting. Conditioned medium was prepared in normal FBS (10%) medium or low FBS (2%) medium. **(C)** After stimulation, conditioned medium was removed, and the mesothelial cells were returned to normal culture medium for another 72 h, after which the MMT markers were measured by Western blotting. **(D)** Wound-healing assays were used to investigate the migratory ability of mesothelial cells after being treated by conditioned medium. **(E)** Cytokine antibody arrays. Samples of supernatant from three ovarian cancer cell lines, namely, ES2, SKOV3, and HEY cells, were collected. On the membrane, each pair of dots represents positive cytokines and highly expressed cytokines are indicated above. Three pairs of positive controls are located at the top right, top left and bottom left corners. The negative control is located at the bottom right corner. Data were calculated by the intensity of each pair of dots. **(F)** ELISA data confirmed the abundance of PAI-1 in conditioned media from array results, together with the other cell lines. Low FBS (2%) culture medium was used as a control. **(G)** Western blotting data confirmed the PAI-1 expression from the array results. The other five cell lines were chosen for comparison. GAPDH was used as an internal reference. **(H)** Wound-healing assay data using mesothelial cells treated with recombinant PAI-1. Representative photos of view are shown. **Abbreviation:** GRO-α: growth-regulated oncogene alpha; PDGF-AA: platelet-derived growth factor AA subunit; DKK-1: dickkopf-related protein 1; uPAR: urokinase receptor; TSP-1: thrombospondin-1; GDF-15: growth differentiation factor-15. Data are presented as the mean ± SD. Statistics are shown as $*P < 0.05$; $**P < 0.01$.

Figure 2. An oncogenic feedback loop is formed after PAI-1-triggered CAM formation. (A) Transwell assays of cell migration and invasion. After treatment with ES2 cell conditioned medium (CM+) or recombinant PAI-1 (PAI-1+), CAMs were formed, and CAM supernatant was collected to treat ES2 and SKOV3 cells. Normal HPMC medium was used as a control. **(B)** Statistics for the Transwell assays. **(C)** Cytokine antibody arrays to identify potential candidates in the CAM supernatant compared with HPMC medium as a control. IL-8, CXCL5, lipocalin-2, and GDF-15 were top four up-regulated cytokines (red). Besides, IL-6 and TNFα showed no significant differences (blue). Each pair of dots was calculated by intensity. **(D)** ELISA to confirm the secretion of IL-8 and CXCL5 from CAMs stimulated by recombinant PAI-1 or by ES2 cell supernatant. Three independent experiments were performed. Photos of Transwell assays were taken from three fields of view and representative photos are shown here. **Abbreviation:** GDF-15: growth differentiation factor-15; IL-6: interleukin-6; TNFα: tumor-necrosis-factor alpha. Data are presented as the mean ± SD. Statistics are shown as $*P < 0.05$; $**P < 0.01$.

Figure 3. The nuclear NFκB pathway in CAMs is activated by PAI-1. (A) Predicted NFκB binding sites to the promoter regions of both IL-8 and CXCL5 share the same sequence: GGAATTTCC. **(B)** After being treated with conditioned medium (CM), primary mesothelial cell lysates were collected for Western blotting. The nuclear and cytoplasmic protein expression of NFκB components, together with their upstream regulators, the IKKs, were investigated. LDH and Lamin B were used as cytoplasmic and nuclear references, respectively. To confirm equal protein loading, β-actin was used as a reference control. Nuclear p65, ser536, and IKKβ were activated. **(C)** Further confirmation by recombinant PAI-1 on four independent samples of primary mesothelial cells. Nuclear p65, ser536, and IKKβ were investigated, with the densitometry graph for quantification and statistics of all blots. The intensity of each blot was calculated by ImageJ software. **(D)** Upstream

regulatory mechanism of the NFκB pathway by Western blotting. Nuclear IKKβ was activated by PAI-1.Thus, an IKKβ-specific inhibitor PS1145 was used to treat the HPMCs (20 μM for a 24 h pretreatment of HPMCs), followed by recombinant PAI-1 treatment. **(E)** With PAI-1 expression in conditioned medium inhibited by RNAi (**Supplementary Fig. S1**), nuclear p65, ser536, and IKKβ in mesothelial cells were further investigated. **(F)** Results of a co-immunoprecipitation assay conducted by incubating antibodies of p65, ser536, and IKK-β with nuclear lysates of mesothelial cells stimulated by conditioned medium or recombinant PAI-1. The binding effects between each of the two components were compared by antibody probing and re-probing. **Abbreviations:** CM: conditioned medium; PAI-1: recombinant PAI-1; sh1: ES2-sh1-PAI-1-luc cells; sh2: ES2-sh2-PAI-1-luc cells; IKKα: inhibitor of nuclear factor kappa-B kinase subunit alpha; IKKβ: inhibitor of nuclear factor kappa-B kinase subunit beta; p65: nuclear factor NF-kappa-B subunit p65; p50: nuclear factor NF-kappa-B subunit p50; ser536: phosphorylate p65 at serine 536; IκBα: NFKB inhibitor alpha; LDH: lactate dehydrogenase; Lamin B: nuclear lamina protein B. Three independent experiments were performed. Data are presented as the mean ± SD. Statistics are shown as $*P < 0.05$; $**P < 0.01$.

Figure 4. PAI-1 stimulation transcriptionally increases nuclear NFκB recruitment to the promoters of IL-8 and CXCL5. (A) NFκB activity analysis via the luciferase reporter assay. The pTAL-NFκB vector (Firefly Luc) and pRL-TK vector (Renilla Luc) were used for co-transfection. Luciferase activity was calculated as Firefly Luc value/Renilla Luc value. **(B)** A list of predicted NFκB binding sites in the promoter regions of IL-8, CXCL5, TNFα and IL-6. **(C)** The mRNA expression of IL-8, CXCL5, TNFα and IL-6 in CAMs after PAI-1 stimulation for 48 and 72 h. HPMCs were used as a control. GAPDH was used for normalization. **(D)** Recruitment effects of p65, ser536, and IKKβ on the promoters of endogenous IL-8, CXCL5, TNFα, and IL-6 were analyzed by ChIP qPCR in mesothelial cells treated with

recombinant PAI-1. **(E)** To analyze whether IKKβ activity was required for IL-8 and CXCL5 promoter recruitment, the IKKβ inhibitor PS1145 was added to mesothelial cells for 24 h pretreatment. Afterwards, a ChIP assay was performed. The results of ChIP qPCR were calculated from at least three independent repeats. Calculation was by the method of normalization to both input (1%) and IgG values. **Abbreviation:** PAI-1: recombinant PAI-1. All data are presented as the mean ± SD. Statistics are shown as $*P < 0.05$; $**P < 0.01$.

Figure 5. Secretory PAI-1 activates CAM formation to accelerate ovarian cancer metastasis in both *ex vivo* and *in vivo* models. (A) Graphic explanation for the *ex vivo* model: after spreading cancer cells onto human peritoneal omentum pieces, the *ex vivo* system was cultured in RPMI-1640 medium under normal conditions. Three replicates of each group were calculated. **(B)** ES2-sh1-PAI-1-luc cells (ES2-sh1) and ES2-sh2-PAI-1-luc cells (ES2-sh2), with luciferase constantly expressed, were seeded and cultured for 3 days. The status of cancer cell dissemination was observed and quantified under the IVIS. **(C)** Extended *ex vivo* assay for 7 days. ES2-sh1 was chosen due to its high level of inhibition. For further confirmation of PAI-1's role, recombinant PAI-1 was also used. **(D)** The luciferase reporter assay was used to identify successfully implanted ES2 cells by detecting stably expressed luciferase. On day 7, after IVIS imaging, the omentum was washed thoroughly and digested by trypsin. Then, cell extracts were collected for the luciferase reporter assay. **(E)** Peritoneal metastases of ovarian cancer in the mice in each group (n = 6) were observed every 3 days using the IVIS. The bioluminescence value of the region of interest (ROI) was used to calculate the metastatic tumor-bearing burden of each mouse. The most representative mouse for each group is shown. **(F)** After day 15, mice were sacrificed and the peritoneal resident tumor nodules in the mesenteria in each group were directly observed. **(G)** Ascites volumes in each group of mice were compared. **Abbreviations:** ES2: ES2-sh-control-luc cells; Meso: primary mesothelial

cells; ES2-sh1: ES2-sh1-PAI-1-luc cells; ES2-sh2: ES2-sh2-PAI-1-luc cells. Replicates of each group (IVIS imaging) of both *in vivo* and *ex vivo* models are presented in **Supplementary Fig. S3-4.** All data are shown as the mean ± SD. Statistics are shown as $*P < 0.05$; $**P < 0.01$.

Figure 6. PAI-1 predicts poor clinical outcomes for ovarian cancer patients. (A) Intensity of PAI-1 expression in 67 tissue samples. Two major pathological types of ovarian cancer are presented here: serous adenocarcinoma and clear-cell carcinoma. PAI-1 expression intensity was scored as follows: negative (0), weak (1), intermediate (2), and strong (3). Expression involved the *H*-score method. **(B)** Kaplan-Meier survival analysis of PAI-1 for the overall survival rate of the 67 patients. **(C)** mRNA levels of PAI-1 in ovarian cancer tissues (586 cases) compared with that of normal ovary tissues (8 cases). **(D)** In the 586 cases of ovarian cancer tissues, 363 (61.95%) cases showed high PAI-1 expression and 223 (38.05%) cases showed low PAI-1 expression. **(E)** Comparison of PAI-1 expressions between early-stage (43 cases) and advanced-stage (520 cases) patients (Because 23 patients did not have detailed information on the FIGO stage, 563 cases were compared)**. (F)** Survival analysis of 562 patients in terms of PAI-1 expression, by the Kaplan-Meier method (1 case had no survival data). **(G)** ELISA to investigate the expression of PAI-1 between benign (9 cases) and malignant (13 cases) ascites. Data of PAI-1 mRNA expression (TCGA database) are presented as $\log_2$ calculations. Data are presented as the mean ± SD. Statistics are shown as $*P < 0.05$; $**P < 0.01$.

Tables and figures

Table 1. Association between protein expression of PAI-1 and the clinical features of ovarian cancer patients.

Characteristics	Cases number	PAI-1 expression		*Chi*-square	*P* value
		High	Low		
Total	67				
Age					
<50		13	13	0.238	0.626
⩾50		23	18		
FIGO stage					
I, II		19	24	2.967	0.085
III, IV		17	7		
Tumor grade					
G1, G2		19	21	1.550	0.213
G3		17	10		
Histological type					
Clear-cell		19	19	0.492	0.483
Serous and others		17	12		
Reccurence					
YES		21	7	6.563	**0.010** *
NO		15	24		
Lymph node status					
N_0		24	24	0.948	0.330
N_1 or N_x		12	7		
Peritoneal dissemination					
YES		22	9	6.895	**0.009** **
NO		14	22		
Ascites Volume					
Severe (⩾500 mL)		12	7	0.948	0.330
< 500 mL		24	24		
Tumor size					
⩾ 10 cm		24	22	0.143	0.705
< 10 cm		12	9		
CA-125					
High (> 35)		30	20	3.115	0.078
Low (≤ 35)		6	11		

* $P < 0.05$ is considered as significantly different. $P < 0.01$ is presented as **.

Figure 1

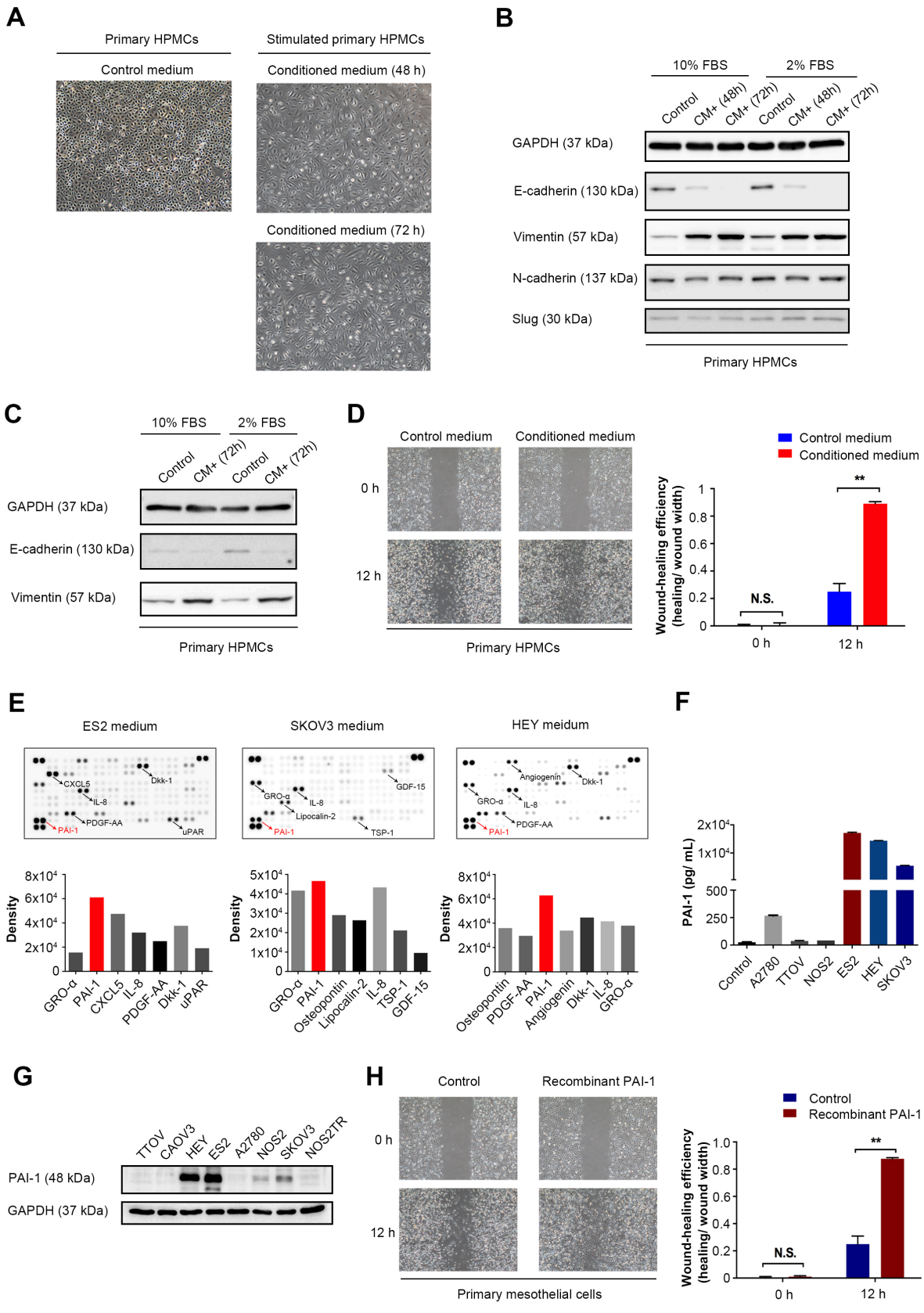
A
Primary HPMCs
Stimulated primary HPMCs
Control medium
Conditioned medium (48 h)
Conditioned medium (72 h)
B
10% FBS
2% FBS
Control
CM+ (48h)
CM+ (72h)
Control
CM+ (48h)
CM+ (72h)
GAPDH (37 kDa)
E-cadherin (130 kDa)
Vimentin (57 kDa)
N-cadherin (137 kDa)
Slug (30 kDa)
Primary HPMCs
C
10% FBS
2% FBS
Control
CM+ (72h)
Control
CM+ (72h)
GAPDH (37 kDa)
E-cadherin (130 kDa)
Vimentin (57 kDa)
Primary HPMCs
D
Control medium
Conditioned medium
0 h
12 h
Primary HPMCs
Control medium
Conditioned medium
Wound-healing efficiency (healing/ wound width)
**
N.S.
0 h
12 h
E
ES2 medium
SKOV3 medium
HEY meidum
CXCL5
Dkk-1
IL-8
PDGF-AA
PAI-1
uPAR
GRO-α
IL-8
Lipocalin-2
GDF-15
PAI-1
TSP-1
Angiogenin
Dkk-1
GRO-α
IL-8
PDGF-AA
PAI-1
Density
GRO-α
PAI-1
CXCL5
IL-8
PDGF-AA
Dkk-1
uPAR
Density
GRO-α
PAI-1
Osteopontin
Lipocalin-2
IL-8
TSP-1
GDF-15
Density
Osteopontin
PDGF-AA
PAI-1
Angiogenin
Dkk-1
IL-8
GRO-α
F
PAI-1 (pg/ mL)
Control
A2780
TTOV
NOS2
ES2
HEY
SKOV3
G
TTOV
CAOV3
HEY
ES2
A2780
NOS2
SKOV3
NOS2TR
PAI-1 (48 kDa)
GAPDH (37 kDa)
H
Control
Recombinant PAI-1
0 h
12 h
Primary mesothelial cells
Control
Recombinant PAI-1
Wound-healing efficiency (healing/ wound width)
**
N.S.
0 h
12 h

Figure 2

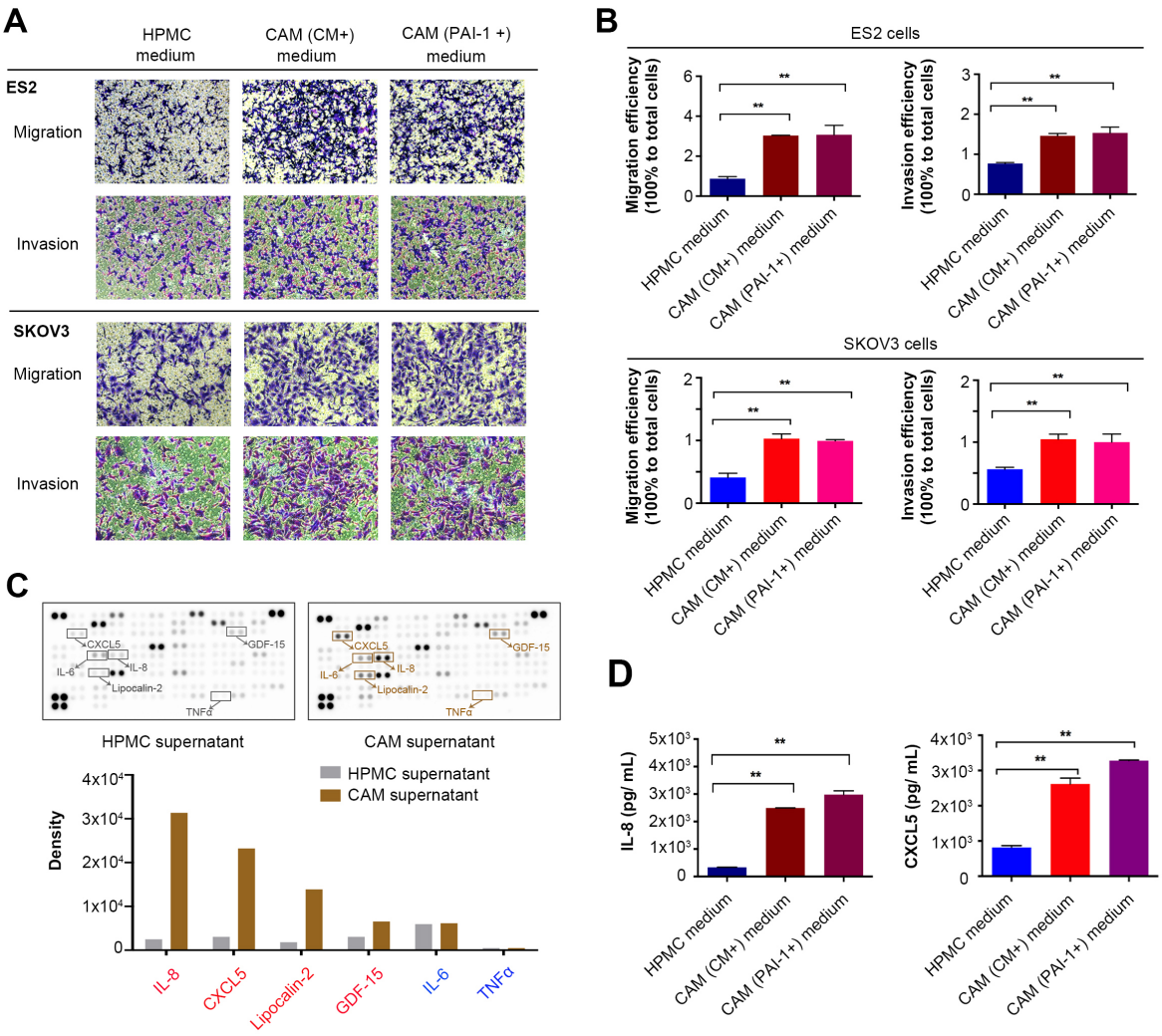
A
HPMC medium
CAM (CM+) medium
CAM (PAI-1 +) medium
ES2
Migration
Invasion
SKOV3
Migration
Invasion
B
ES2 cells
Migration efficiency (100% to total cells)
Invasion efficiency (100% to total cells)
HPMC medium
CAM (CM+) medium
CAM (PAI-1+) medium
SKOV3 cells
C
CXCL5
GDF-15
IL-6
IL-8
Lipocalin-2
TNFα
HPMC supernatant
CAM supernatant
Density
D
IL-8 (pg/ mL)
CXCL5 (pg/ mL)

Figure 3

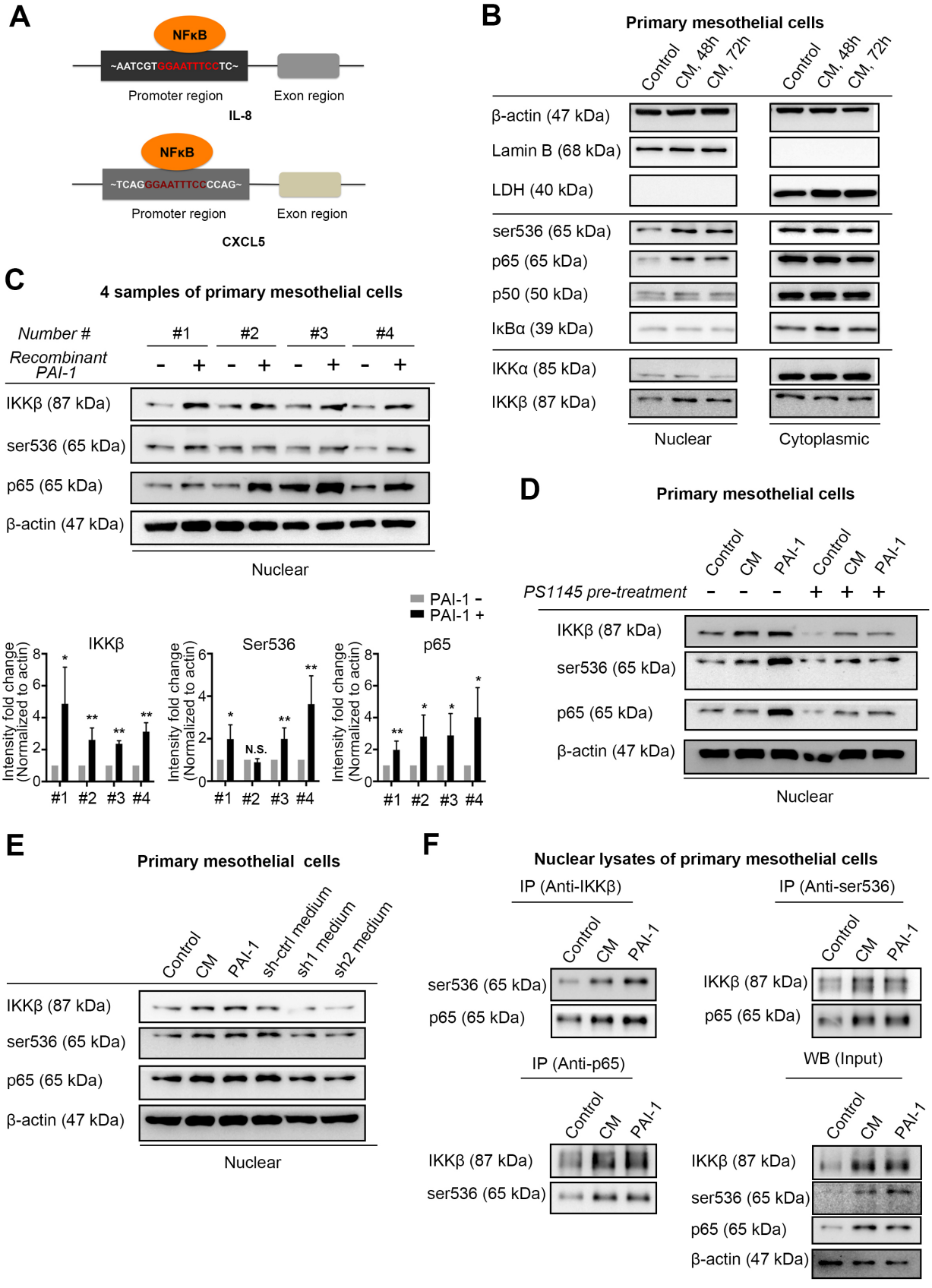
A
NFκB
~AATCGTGGAATTTCCTC~
Promoter region
Exon region
IL-8
NFκB
~TCAGGGAATTTCCCCAG~
Promoter region
Exon region
CXCL5
B
Primary mesothelial cells
Control
CM, 48h
CM, 72h
Control
CM, 48h
CM, 72h
β-actin (47 kDa)
Lamin B (68 kDa)
LDH (40 kDa)
ser536 (65 kDa)
p65 (65 kDa)
p50 (50 kDa)
IκBα (39 kDa)
IKKα (85 kDa)
IKKβ (87 kDa)
Nuclear
Cytoplasmic
C
4 samples of primary mesothelial cells
Number #
#1
#2
#3
#4
Recombinant PAI-1
- + - + - + - +
IKKβ (87 kDa)
ser536 (65 kDa)
p65 (65 kDa)
β-actin (47 kDa)
Nuclear
PAI-1 -
PAI-1 +
IKKβ
Ser536
p65
Intensity fold change (Normalized to actin)
N.S.
#1 #2 #3 #4
D
Primary mesothelial cells
Control
CM
PAI-1
Control
CM
PAI-1
PS1145 pre-treatment
- - - + + +
IKKβ (87 kDa)
ser536 (65 kDa)
p65 (65 kDa)
β-actin (47 kDa)
Nuclear
E
Primary mesothelial cells
Control
CM
PAI-1
sh-ctrl medium
sh1 medium
sh2 medium
IKKβ (87 kDa)
ser536 (65 kDa)
p65 (65 kDa)
β-actin (47 kDa)
Nuclear
F
Nuclear lysates of primary mesothelial cells
IP (Anti-IKKβ)
Control
CM
PAI-1
ser536 (65 kDa)
p65 (65 kDa)
IP (Anti-ser536)
Control
CM
PAI-1
IKKβ (87 kDa)
p65 (65 kDa)
IP (Anti-p65)
Control
CM
PAI-1
IKKβ (87 kDa)
ser536 (65 kDa)
WB (Input)
Control
CM
PAI-1
IKKβ (87 kDa)
ser536 (65 kDa)
p65 (65 kDa)
β-actin (47 kDa)

Figure 4

A

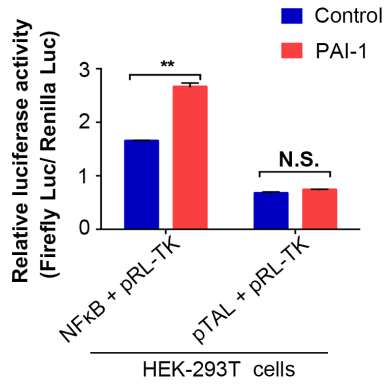

B

Gene name	Predicted NFκB binding sequence
IL-8	GGAATTTCC
CXCL5	GGAATTTCC
TNFα	GGAATTCCCA
IL-6	GGATTTCAG

C

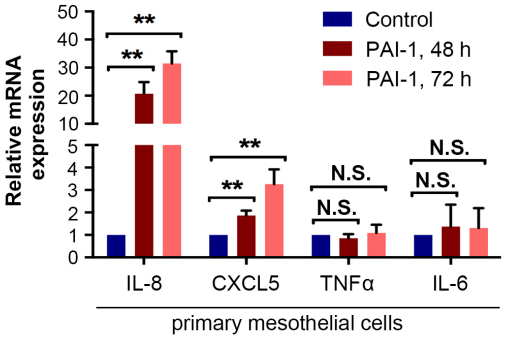

D

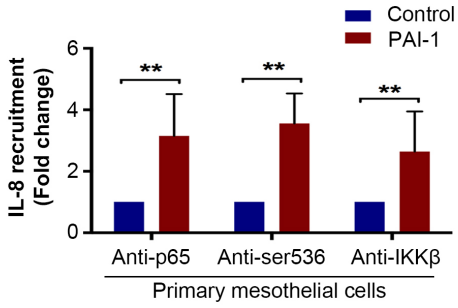

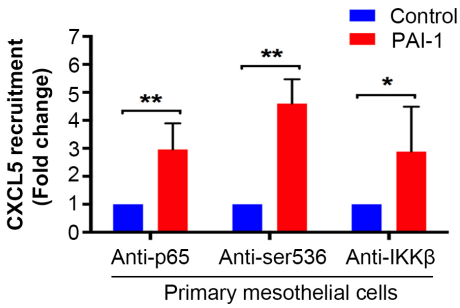

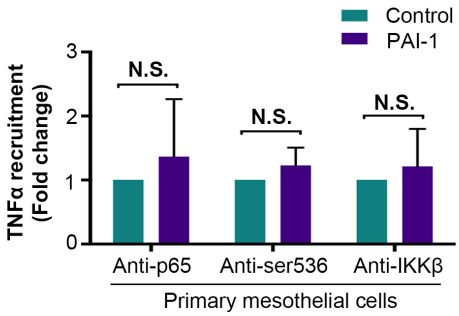

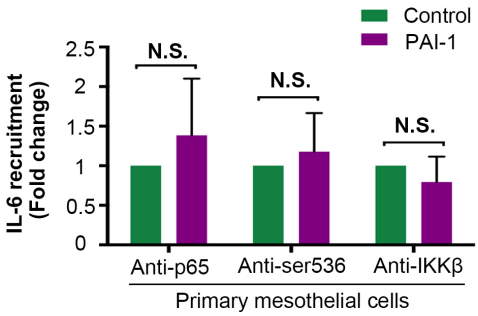

E

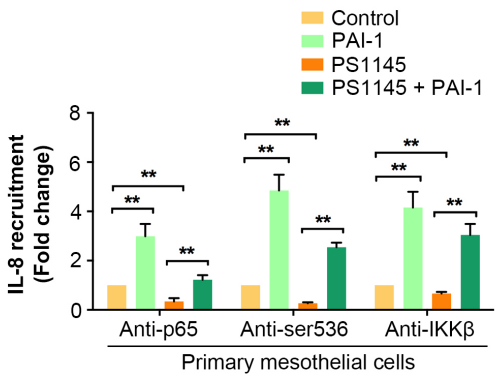

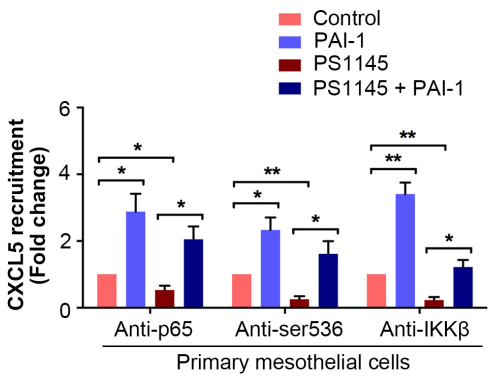

Figure 5

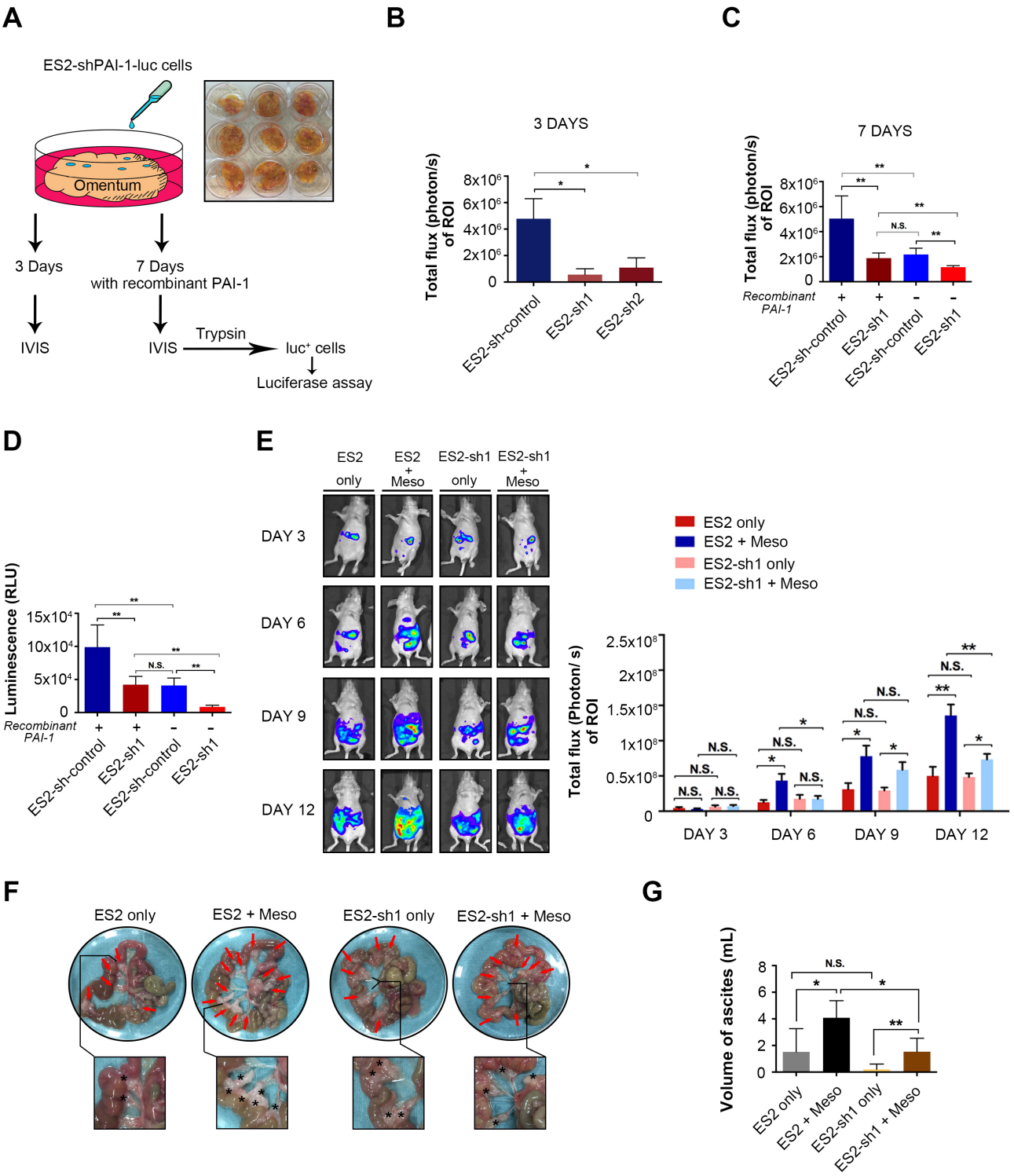
A
ES2-shPAI-1-luc cells
Omentum
3 Days
7 Days
with recombinant PAI-1
IVIS
IVIS
Trypsin
luc+ cells
Luciferase assay
B
3 DAYS
Total flux (photon/s) of ROI
8x10^6
6x10^6
4x10^6
2x10^6
0
ES2-sh-control
ES2-sh1
ES2-sh2
C
7 DAYS
Total flux (photon/s) of ROI
Recombinant PAI-1
ES2-sh-control
ES2-sh1
ES2-sh-control
ES2-sh1
D
Luminescence (RLU)
15x10^4
10x10^4
5x10^4
0
Recombinant PAI-1
ES2-sh-control
ES2-sh1
ES2-sh-control
ES2-sh1
E
ES2 only
ES2 + Meso
ES2-sh1 only
ES2-sh1 + Meso
DAY 3
DAY 6
DAY 9
DAY 12
Total flux (Photon/ s) of ROI
2.5x10^8
2x10^8
1.5x10^8
1x10^8
0.5x10^8
0
DAY 3
DAY 6
DAY 9
DAY 12
F
ES2 only
ES2 + Meso
ES2-sh1 only
ES2-sh1 + Meso
G
Volume of ascites (mL)
8
6
4
2
0
ES2 only
ES2 + Meso
ES2-sh1 only
ES2-sh1 + Meso

Figure 6

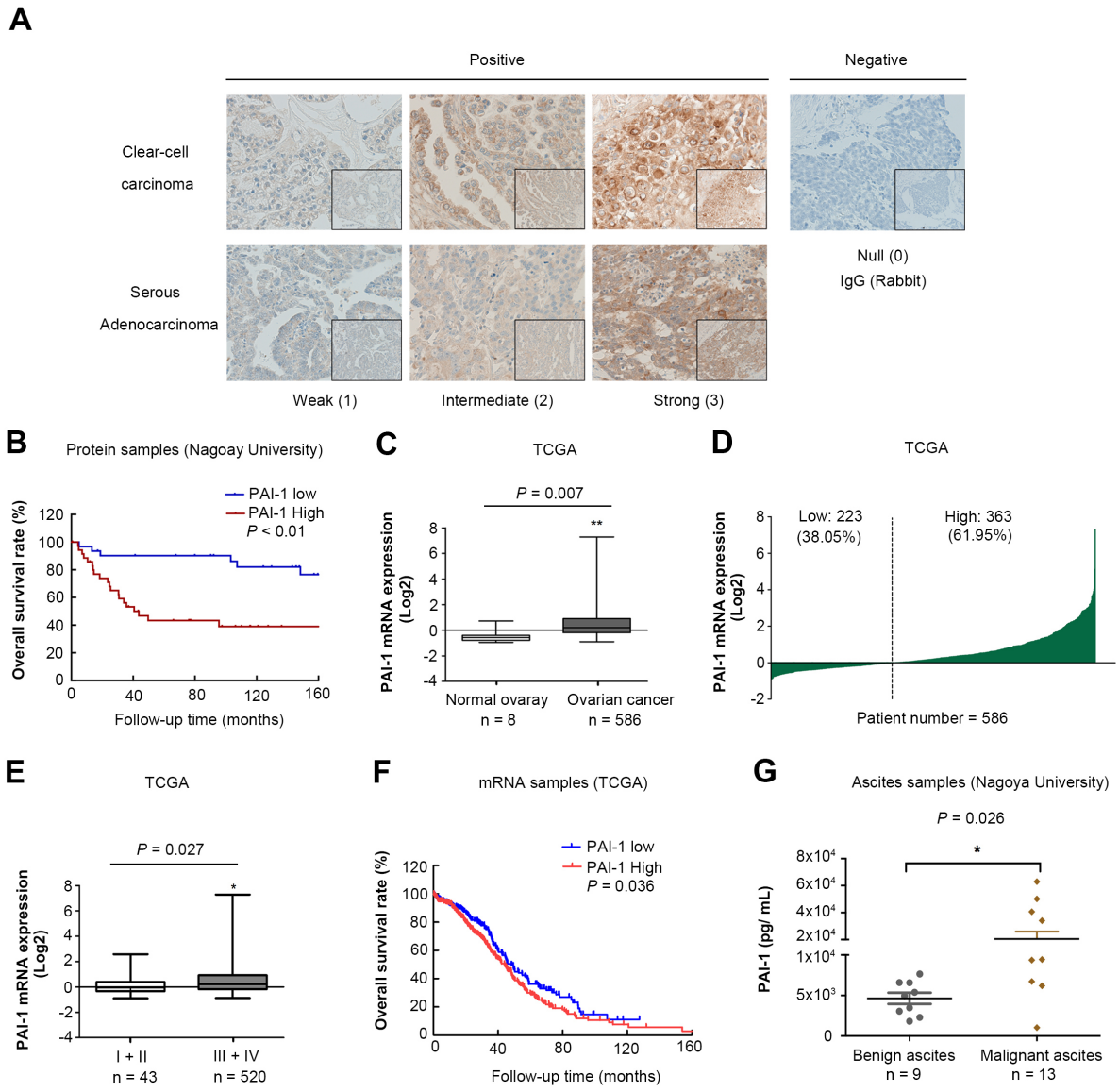
A
Positive
Negative
Clear-cell carcinoma
Serous Adenocarcinoma
Null (0)
IgG (Rabbit)
Weak (1)
Intermediate (2)
Strong (3)
B
Protein samples (Nagoay University)
PAI-1 low
PAI-1 High
P < 0.01
Overall survival rate (%)
Follow-up time (months)
C
TCGA
P = 0.007
PAI-1 mRNA expression (Log2)
Normal ovaray
n = 8
Ovarian cancer
n = 586
D
TCGA
Low: 223
(38.05%)
High: 363
(61.95%)
PAI-1 mRNA expression (Log2)
Patient number = 586
E
TCGA
P = 0.027
PAI-1 mRNA expression (Log2)
I + II
n = 43
III + IV
n = 520
F
mRNA samples (TCGA)
PAI-1 low
PAI-1 High
P = 0.036
Overall survival rate (%)
Follow-up time (months)
G
Ascites samples (Nagoya University)
P = 0.026
PAI-1 (pg/ mL)
Benign ascites
n = 9
Malignant ascites
n = 13